Lithos 106 (2008) 12–24

Contents lists available at ScienceDirect

Lithos

journal homepage: www.elsevier.com/locate/lithos

Comparison of the Daluxiang and Maoniuping carbonatitic REE deposits with Bayan Obo REE deposit, China

Cheng Xu [a,*], Ian H. Campbell [b], Jindrich Kynicky [c], Charlotte M. Allen [b], Yanjing Chen [d], Zhilong Huang [a], Liang Qi [a]

[a] Laboratory of Materials of the Earth's Interior and Geofluid Processes, Institute of Geochemistry, Chinese Academy of Sciences, Guiyang 550002, China
[b] Research School of Earth Sciences, Australian National University, Canberra, Australia
[c] Department of Geology and Pedology, Mendel University of Agriculture and Forestry, Brno, Czech Republic
[d] Department of Geology, Peking University, Beijing 100871, China

ARTICLE INFO

Article history:
Received 8 February 2008
Accepted 7 June 2008
Available online 19 June 2008

Keywords:
Carbonatites
Carbonate mineral
REE mineralization
Daluxiang
Maoniuping
Bayan Obo

ABSTRACT

Although carbonatites potentially contain a larger concentration of rare earth elements (REEs) than any rock type, the origin of the REE mineralization in the world's largest Bayan Obo carbonatite-related deposit is still disputed. In order to clarify the mechanism of REE mineralization, carbonatite samples from three large REE deposits in China, Daluxiang, Maoniuping and Bayan Obo were compared. The REE minerals in Daluxiang and Maoniuping carbonatites show constant light REE (LREE) enrichment (chondrite normalized $(La/Nd)_N$ ratios>1), whereas those in Bayan Obo H8 dolomite marbles show variable $(La/Nd)_N$ ratios. The REE abundances and patterns of the REE minerals in Maoniuping carbonatites are similar to those in the barite, calcite and thread vein-hosted ores. The calcites in Daluxiang and Maoniuping carbonatites are characterized by enrichments of Pb, Sr and REEs, which is consistent with an igneous origin. They have similar REE contents and patterns to the corresponding bulk rocks, suggesting that these carbonatites are calcite-rich cumulates. During crystallization and accumulation of calcites, the REEs become enriched in carbonatite-expelled fluids because of the very low partition coefficients for these elements between carbonate minerals and melt. These fluids interact with the country rocks to produce fluorite-rich REE mineralization. The fluorites in Daluxiang and Maoniuping deposits are characterized by high Sr contents and REE patterns that vary from LREE enriched to LREE depleted. The former has relatively higher Sr and lower heavy REE (HREE) concentrations than those in Maoniuping, which is consistent with the differences found in carbonatites and calcites from the two locations. In addition, the high MnO, Sr and REE contents of dolomites in REE–Nb–Fe host H8 dolomite marble in Bayan Obo support the hypothesis that the rock is of igneous origin. In situ analyses show compositional differences between coarse- and fine-grained dolomites. The latter has higher Nb and LREEs, and lower FeO and $^{207}Pb/^{206}Pb$ and $^{208}Pb/^{206}Pb$ ratios. Our data confirm previous interpretations of the complex, multistage nature of REE and Nb mineralization at Bayan Obo, in which the ore is produced by reaction between carbonatite-derived fluids and the ore host dolomite marbles. This hypothesis is supported by the age of adjacent carbonatite dykes, which have the same age range as ore formation. A similar REE mineralization model is proposed for the Daluxiang and Maoniuping carbonatite deposits.

1. Introduction

Rare earth elements (REEs) are important materials in high-technology industry (e.g. permanent magnets, microwave dielectrics, steel, and ceramics). As a consequence, there is an increased interest in exploring for new sources of these elements. Carbonatites contain the highest concentration of REEs of any igneous rock, and are therefore good targets for REE exploration. However, these concentrations are usually small in volume and only a few economic deposits have been found, including Mountain Pass, USA (e.g. Mariano, 1989), Tundulu and Kangankunde in Malawi (e.g. Wall and Mariano, 1996), and Bayan Obo (e.g. Ren, 1985), Maoniuping (e.g. Yuan et al., 1995), and Daluxiang (e.g. Li, 2005) in China. The largest production and economic value in carbonatites result from apatite mining in Europe, Brazil, and South Africa, followed by Cu mining from Phalaborwa (Mariano, 1989). The genesis of the world's largest REE deposits related with carbonatites in Bayan Obo is still disputed (e.g. Chao et al., 1992; Yuan et al., 1992). The previous studies were mainly focused on the analyses of carbonatite whole rock (e.g. Andrade et al., 1999; Yang et al., 2003), gangue mineral fluorite (e.g. Williams-Jones et al., 2000; Xu et al., 2001, 2003b), apatite (e.g. Campbell and Henderson, 1997) and REE minerals (e.g. Smith et al.,

* Corresponding author. Institute of Geochemistry, Chinese Academy of Sciences, 46 Guanshui Road, Guiyang 550002, Guizhou Province, China. Tel.: +86 851 5895194; fax: +86 851 5891117.
E-mail address: xucheng1999@hotmail.com (C. Xu).

0024-4937/$ – see front matter © 2008 Elsevier B.V. All rights reserved.
doi:10.1016/j.lithos.2008.06.005

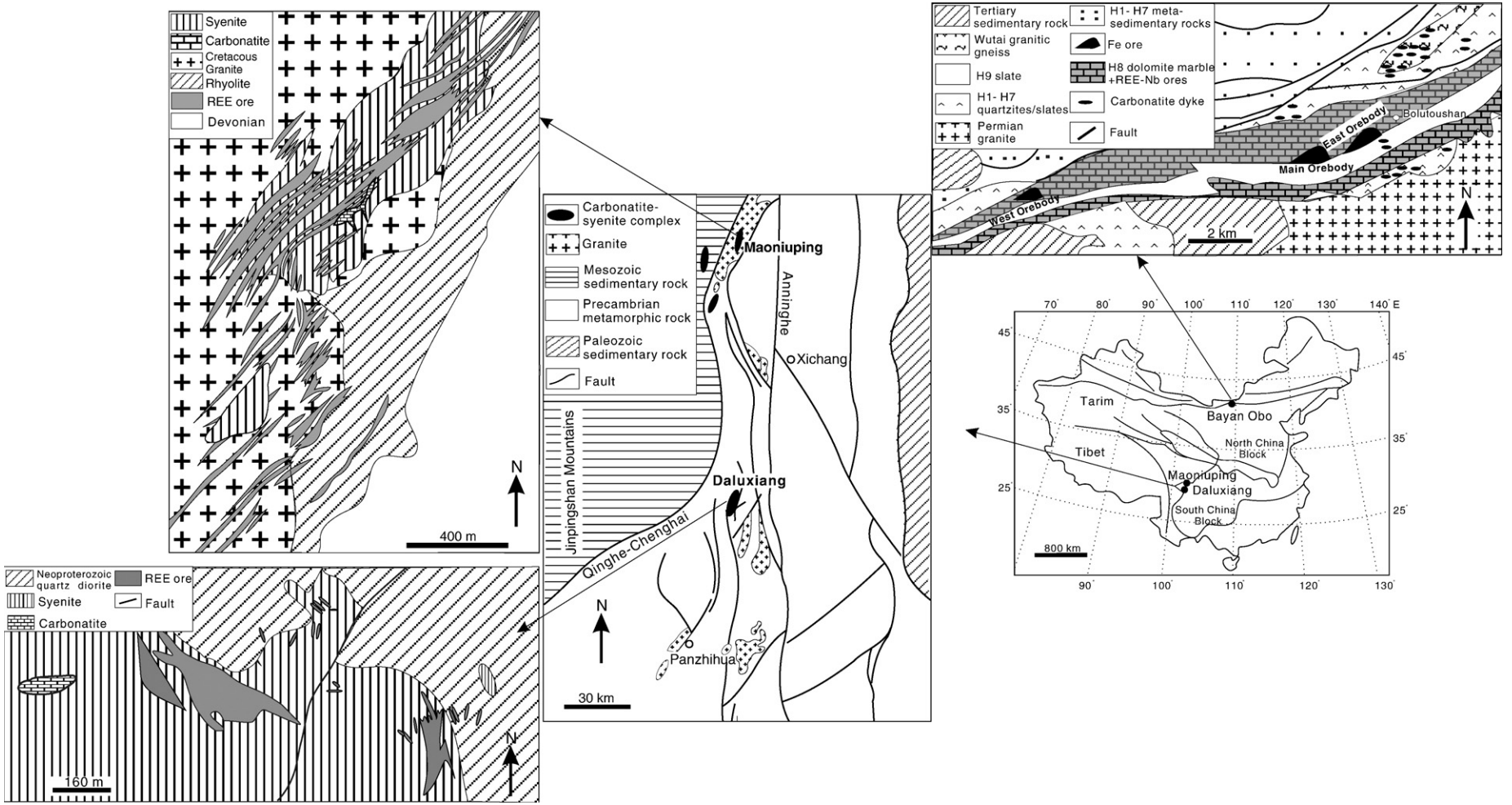

Fig. 1. Geological sketch of the Daluxiang, Maoniuping and Bayan Obo REE deposits (modified after Pu, 1988; Yuan et al., 1992, 1995; Tao et al., 1998; Li, 2005).

1999, 2000), and some silicate phases associated with carbonatites and orebodies such as aegirine, biotite and amphibole (e.g. Smith, 2007). However, the mineral chemistry of carbonates, the most abundant minerals in carbonatites, has been neglected.

This paper reports compositions of carbonatites and fluorites associated with REE ores measured by solution ICPMS (Inductively Coupled Plasma Mass Spectrometry) and of REE minerals and carbonates determined in situ by electron microprobe and LA (Laser Ablation)-ICPMS. The samples were collected from three REE deposits in China, namely Bayan Obo, Daluxiang and Maoniuping. The Bayan Obo deposit in Inner Mongolia is the largest REE deposit in the world, and the Maoniuping and Daluxiang in Sichuan Province are also large REE deposits. Our aim is to explore the relationship between REE mineralization and carbonatites.

2. Geological features

The Daluxiang and Maoniuping deposits are located on the northwest and central margin of the Panxi (Panzhihua-Xichang) region, respectively (Fig. 1). The area underwent a complicated tectonic evolution from Proterozoic lithospheric accretion, through the Paleozoic–Mesozoic continental margin, followed by a Cenozoic collision orogeny (Zhang et al., 1988). In the Panxi region, carbonatites are associated with syenites, and comprise a 270-km-long, NS-trending belt of carbonatite-alkalic complexes (Fig. 1), which intrude the Proterozoic crystalline basement rocks and Paleozoic–Mesozoic sedimentary sequences. The belt is bounded by the Qinghe–Chenghai and Anninghe strike-slip faults, whereas the individual complexes in this belt were controlled by second-order strike-slip faults. Carbonatites occur as sills, dykes and stocks within the syenite intrusions. Presently, eight REE deposits are found associated with these carbonatite-syenite complexes (Pu, 2001).

2.1. Daluxiang

At Daluxiang, a 1400 m long and 600–800 m wide complex consists of syenite and carbonatite veins, which intrude a Proterozoic quartz diorite pluton. The carbonatite is medium- to coarse-grained, consisting of calcite (Fig. 2A) and subordinate microcline, quartz, arfvedsonite, barium-rich celestine, strontiobarite, fluorite, aegirine,

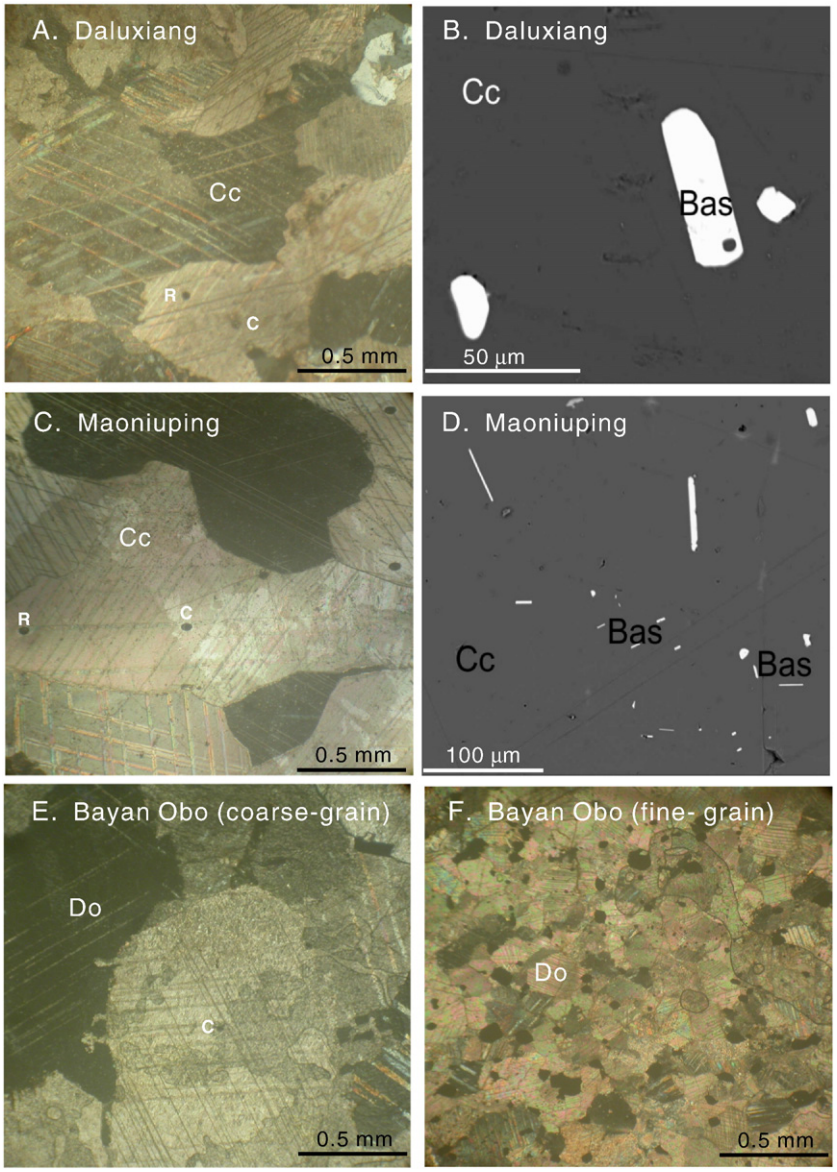

Fig. 2. Photomicrographs of carbonatites (A, C, E, F; crossed-polarized transmitted light) and REE minerals (B, D; backscattered electron image). Cc, calcite; Bas, bastnäsite-(Ce); Do, dolomite; R, C, rim and core of spots for analyses.

Table 1
Representative analysis of REE minerals in Daluxiang and Maoniuping REE deposits

Daluxiang						Maoniuping					
Sample	Bt-1	Bt-2	Pt	Mt-1	Mt-2	Bt-1	Bt-2	Bt-3	Pt	Mt-1	Mt-2
SiO_2	0.13	0.14	0.12	0.10	0.52	0.11	0.13	0.13	0.08	0.44	0.25
FeO	0.13	0.05	0.07	bdl	bdl	bdl	bdl	bdl	bdl	bdl	bdl
CaO	1.48	1.58	10.18	0.55	0.19	0.11	0.09	0.15	9.56	0.46	0.69
P_2O_5	bdl	bdl	bdl	28.68	27.51	0.04	bdl	bdl	bdl	28.36	28.19
Y_2O_3	0.21	0.38	1.82	0.12	0.05	bdl	bdl	0.02	bdl	0.18	0.19
La_2O_3	18.75	18.63	12.94	22.21	21.73	25.15	21.77	27.69	19.44	22.96	22.79
Ce_2O_3	33.55	33.4	24.61	34.03	34.89	31.15	32.86	30.33	28.11	34.58	33.79
Pr_2O_3	3.47	3.38	2.66	2.57	2.95	2.45	2.60	2.07	2.30	2.73	2.92
Nd_2O_3	11.61	11.89	11.44	7.75	8.36	6.33	7.86	5.30	6.02	8.66	8.41
Sm_2O_3	1.18	1.15	2.40	0.73	0.99	0.57	0.80	0.55	0.63	0.82	0.97
Gd_2O_3	0.35	0.63	1.78	0.11	bdl	0.10	0.13	0.13	bdl	0.22	0.39
Dy_2O_3	0.12	0.14	0.29	bdl	bdl	bdl	bdl	bdl	bdl	0.16	0.11
ThO_2	bdl	bdl	bdl	0.13	bdl	0.30	0.12	0.16	bdl	0.18	0.21
SO_3	bdl	0.04	bdl	0.09	0.17	bdl	bdl	bdl	bdl	0.16	0.22
CO_2*	19.65	19.71	25.56			20.51	20.47	21.10	25.08		
H_2O*	1.08	1.14	5.23			4.20	4.19	4.32	5.13		
F	6.21	6.11	5.62	bdl	bdl	6.52	6.54	6.35	5.47	bdl	bdl
F=O	−2.61	−2.57	−2.37			−2.75	−2.75	−2.67	−2.30		
Total	95.31	95.80	102.35	97.07	97.36	94.79	94.81	95.63	99.52	99.91	99.13

Bt, bastnäsite-(Ce); Pt, parisite-(Ce); Mt, monazite-(Ce); bdl, below detection limit; CO_2 and H_2O are calculated by charge balance.

apatite, REE minerals and sulfides. Principal REE minerals are fluorocarbonates and monazite [(Ce,La,Nd,Th)PO_4]. Fluorocarbonates occur in aggregates (5–150 μm) that are interlocked with calcite. These aggregates take the form of composite bastnäsite [(Ce,La)(CO_3)F], parisite [(Ce,La)$_2$Ca(CO_3)$_3F_2$] and very fine (less than 5 μm) syntaxial intergrowth of intermediate phases. Bastnäsite-(Ce) occurs also as sporadic fine automorphic crystals in calcite (Fig. 2B). Monazite-(Ce) is in close association with barium-rich celestine and strontiobarite.

Although this area has not been extensively explored, two large orebodies (I, III) have been found, which intrude into the syenites as veins (Fig. 1). The syenites were extensively altered to assemblages derived from aegirine-augitization, fluoritization, carbonatization and bastnäsitization at the contact with ore veins. Using the characteristic mineral associations, the orebodies are divided into three groups (e.g. Li, 2005), (1) pegmatitic bastnäsite-(Ce)–aegirine augite–fluorite–strontiobarite veins (strontiobarite veins); (2) pegmatitic bastnäsite-(Ce)–aegirine augite–fluorite–barium-rich celestine veins (barium-rich celestine veins); (3) thread bastnäsite-(Ce)–aegirine augite–strontiobarite–calcite veins (thread veins). The strontiobarite vein is host lode of the orebody with outcropping width of 80–180 m and length of >400 m. The barium-rich celestine vein is host lode of the III orebody with outcropping width of 26–100 m and length of >200 m. The two orebodies show lens- and irregular vein-shaped and contain 4–10 wt.% REE_2O_3. The thread vein is emplaced around the I orebody and has a width of about 1 m. They have granular and euhedral–subhedral texture and tabular structure, and contain 0.5% REE_2O_3. The reserve of REE_2O_3 in Daluxiang deposit has not been estimated. Importantly, the grades of $SrSO_4$ in Daluxiang deposit range from 25.73% to 27.68%, making it an economic source of Sr.

2.2. Maoniuping

At Maoniuping, a 1400 m long, 260–350 m wide complex consists of carbonatite sills and a syenitic intrusion that intrude a Mesozoic granite (Fig. 1). The carbonatite sills (90–200 m wide) dip steeply northwestwards at 70° and extend downwards for at least 400 m in the syenites (Pu, 1988). The carbonatite is mainly composed of coarse-grained calcite (>1 mm; Fig. 2C), with minor and accessory minerals, which include microcline, aegirine, arfvedsonite, biotite and apatite and REE minerals. The principal REE mineral is bastnäsite-(Ce). The carbonatites contain both large and fine automorphic bastnäsite-(Ce) crystals (Fig. 2D). Parisite-(Ce) and monazite-(Ce) occur as sporadic very fine (less than 15 μm) crystals in calcite.

K–Ar dating of the arfvedsonite gave an age of 31.7±0.7 Ma for the Maoniuping carbonatites (Pu, 2001). The Maoniuping orebodies are

Table 2
Representative EPMA data for calcites in Daluxiang (DLX), Maoniuping (MNP) and dolomites in Bayan Obo (BY) REE deposits

	DLX1-1	DLX1-2	DLX1-3	DLX2-1	DLX2-2	DLX4-1	DLX4-2	DLX5-1	DLX5-2	DLX5-3	DLX29-1	DLX29-2	MNP1-1	MNP1-2	MNP1-3	MNP3-1	MNP3-2
MgO	0.07	0.05	0.28	0.03	0.16	0.07	0.06	0.06	bdl	0.09	0.14	0.14	0.24	0.21	0.22	0.24	0.25
CaO	51.91	53.61	54.25	55.59	54.35	52.24	54.84	51.65	52.23	51.46	53.63	55.50	55.31	53.75	54.76	53.00	53.18
MnO	0.34	0.16	0.48	0.28	0.50	0.35	0.37	0.26	0.25	0.31	0.51	0.56	1.03	1.15	1.06	0.53	0.59
FeO	0.17	0.06	0.63	0.27	0.47	0.33	0.36	0.24	0.10	0.24	0.38	0.37	0.60	0.59	0.66	0.40	0.44
SrO	3.71	2.36	1.23	1.50	1.54	2.13	1.26	4.29	3.07	2.74	1.30	1.40	1.39	1.09	0.96	2.53	2.23
CO_2^*	42.70	43.26	44.09	44.63	44.08	42.40	44.09	42.73	42.51	41.99	43.34	44.88	45.26	43.95	44.68	43.5	43.59
Total	98.90	99.50	100.96	102.3	101.10	97.52	100.98	99.23	98.16	96.83	99.30	102.85	103.83	100.74	102.34	100.20	100.28

	MNP4-1	MNP4-2	MNP18-1	MNP18-2	MNP18-3	BY598-1	BY598-2	BY598-3	BY599-1	BY599-2	BY599-3	BY599-4	BY810-1	BY810-2
MgO	0.26	0.29	0.19	0.18	0.16	18.91	19.86	19.16	20.99	17.85	20.26	19.92	14.22	14.43
CaO	54.60	54.33	54.79	54.22	54.86	27.21	26.73	27.63	28.25	28.84	29.63	29.31	27.66	27.21
MnO	1.01	0.77	0.78	0.76	0.76	0.73	0.72	0.91	1.01	0.97	1.02	1.18	1.02	0.99
FeO	0.56	0.67	0.46	0.35	0.41	1.19	0.81	2.02	0.58	1.19	1.12	1.40	9.24	9.01
SrO	1.66	1.48	1.46	2.23	1.80	0.39	0.42	0.17	0.48	0.32	0.41	0.44	0.67	0.44
CO_2^*	44.81	44.47	44.59	44.38	44.71	43.35	43.78	44.48	46.28	43.59	46.87	46.53	43.81	43.43
Total	102.9	102.01	102.27	102.12	102.7	91.78	92.32	94.37	97.59	92.76	99.31	98.78	96.62	95.51

bdl, below detection limit; CO_2 is calculated by charge balance.

Table 3
Fluorite, carbonatite solution ICPMS and carbonate crystal core LA-ICPMS analyses in Daluxiang (DLX), Maoniuping (MNP) and Bayan Obo (BY) REE deposits

Sample	Fluorite	Ba-rich celestine vein	Strontiobarite vein	Later stage	Thread vein	Calcite vein	Barite vein	Later stage		Carbonatite+ Carbonate	WR	C*	WR	C	WR	C
		DLX-27	DLX-30	DLX-33	MNP-6	MNP-25	MNP-135	MNP-22	MNP-23		DLX-1		DLX-2		DLX-4	
		White	Purple	Purple	Purple	Green	White	Purple	Purple			Av. 1		Av.2		Av.4
Rb		0.07	0.09	0.08	bdl	0.43	bdl	0.62	0.06		0.69	0.20	0.12	bdl	0.39	bdl
Sr		7990	13608	6187	3330	5433	3981	2735	4253		23680	12299	12460	7321	24810	11793
Y		112	115	227	133	352	237	260	287		72.7	109	35.7	31.4	54.2	79.3
Zr		0.13	0.67	16.5	0.14	1.38	0.19	3.46	0.36		8.73	0.14	0.44	0.04	5.87	0.02
Nb		0.07	0.24	0.05	0.21	0.56	0.44	1.62	0.26		6.14	0.01	0.28	bdl	2.45	bdl
Ba		5368	777	95.4	723	5433	1591	2735	4253		40320	ie	1065	35.85	30980	103
La		45.2	77.4	30.7	88.2	54.9	148	43.6	39.9		1122	225	212	275	829	301
Ce		66.3	139	81.8	177	119	231	106	105		1898	574	355	416	1342	714
Pr		7.86	15.8	12.4	21.5	17.2	26.3	17.6	17.7		154	69.1	35.2	37.7	111	83.8
Nd		39.2	66.3	69.5	98.0	91.8	129	96.4	102		501	270	116	119	357	322
Sm		9.63	12.3	16.9	19.3	24.6	29.8	28.5	30.4		55.8	47.0	14.6	12.9	42.1	48.6
Eu		2.11	3.67	5.26	5.40	6.75	8.60	7.91	9.55		16.2	13.7	4.35	3.41	11.7	13.1
Gd		7.73	10.9	12.1	17.7	24.4	32.0	25.2	28.6		72.1	31.7	12.7	7.02	27.5	26.8
Tb		1.21	1.50	2.14	1.98	3.55	3.69	3.45	3.87		4.35	3.72	1.34	0.78	2.97	2.97
Dy		5.72	6.20	10.7	10.3	18.3	20.1	17.9	18.6		14.2	18.9	6.10	3.98	10.4	13.6
Ho		1.19	1.32	2.23	1.85	3.70	3.49	3.3	3.8		2.15	3.14	1.23	0.68	1.73	2.19
Er		3.05	3.63	5.92	4.77	9.78	8.85	8.29	9.33		6.09	7.59	3.70	1.72	5.21	5.07
Tm		0.29	0.35	0.60	0.55	1.21	0.93	1.0	1.13		0.67		0.49		0.55	
Yb		1.69	2.14	3.47	3.00	6.61	4.92	5.06	6.31		3.31	4.65	2.68	1.34	2.43	3.77
Lu		0.20	0.26	0.41	0.31	0.80	0.54	0.57	0.79		0.45	0.51	0.39	0.17	0.36	0.47
Hf		0.08	0.10	0.32	0.02	0.15	0.04	0.14	0.14		0.23		0.06		0.14	
Ta		0.04	0.05	0.08	0.01	0.15	0.19	0.11	0.21		0.09	bdl	0.20	bdl	0.07	bdl
Pb		11.1	51.6	1.70	22.3	88.5	49.3	159	125		763	35.2	122	35.0	813	35.9
Th		0.02	0.20	0.01	1.70	0.32	1.24	0.73	1.13		7.83	0.11	0.11	bdl	1.59	bdl
U		0.17	0.68	0.22	0.59	1.37	0.47	2.48	10.2		7.21	1.12	4.04	bdl	3.94	bdl
$^{207}Pb/^{206}Pb$												0.859		0.841		0.877
$^{208}Pb/^{206}Pb$												2.115		2.118		2.137

Sample	WR	C	WR	C	WR	C	WR	C	WR	C*	WR	C*	D	D	D
	DLX-5		DLX-29		MNP-1		MNP-3		MNP-4		MNP-18		BY-598	BY-599	BY-810
		Av.7		Av.4		Av.6		Av.3		Av.1		Av.2	Av.3	Av.5	Av.6
Rb	0.95	0.11	2.21	bdl	0.39	0.04	0.45	0.04	4.47	0.07	0.26	0.01	0.03	0.01	bdl
Sr	23030	12924	46040	10081	10560	9927	9160	9927	8792	7880	14240	9575	2107	2426	3305
Y	102	58.6	53.2	76.4	130	97.3	141	97.3	115	96.3	145	135	9.64	7.62	16.6
Zr	12.7	0.04	3.25	0.01	0.04	0.16	0.30	0.16	43.4	0.01	0.17	0.01	0.12	0.16	0.01
Nb	11.5	bdl	73.4	bdl	0.06	bdl	0.38	bdl	0.99	0.01	0.09	bdl	4.49	1.65	0.12
Ba	16920	170	4574	64.0	981	29.7	1976	29.7	1975	19.8	7652	45.4	85.4	84.1	91.8
La	1527	354	608	251	672	344	411	344	255	191	549	291	163	246	54.0
Ce	2676	621	906	469	1294	689	837	689	642	493	1063	656	266	330	157
Pr	265	62.9	78.6	46.8	127	77.1	82.4	77.1	72.7	61.4	107	78.6	26.9	27.4	22.0
Nd	714	217	259	171	496	293	318	293	299	251	412	318	100	81.2	100
Sm	87.0	28.9	32.5	23.8	71.0	43.7	55.0	43.7	55.1	42.2	64.6	50.6	12.6	7.31	25.1
Eu	24.6	7.80	11.1	6.17	16.8	10.3	14.6	10.3	14.6	10.4	17.0	12.2	3.84	2.35	7.51
Gd	80.2	17.2	25.1	16.4	63.1	29.1	44.3	29.1	35.9	30.0	51.5	35.4	7.40	4.89	16.4
Tb	6.31	1.85	2.48	2.06	6.35	3.48	5.24	3.48	5.0	3.43	5.68	4.09	0.80	0.55	1.66
Dy	21.8	9.13	9.84	11.5	26.9	18.1	25.4	18.1	24.6	18.3	25.0	21.8	3.37	2.48	6.48
Ho	3.30	1.55	1.65	2.23	4.84	3.39	4.78	3.39	4.66	3.30	4.47	4.10	0.44	0.34	0.79
Er	9.39	3.81	4.91	5.95	13.9	9.17	14.7	9.17	14.0	8.98	13.8	11.5	0.80	0.63	1.36
Tm	0.98		0.58		1.77		2.04		1.88		1.85				
Yb	4.65	2.73	2.81	5.14	9.95	8.32	10.9	8.32	9.95	7.97	10.4	10.3	0.31	0.27	0.50
Lu	0.60	0.32	0.36	0.59	1.53	1.11	1.62	1.11	1.46	1.11	1.47	1.40	0.04	0.03	0.05
Hf	0.33		0.13		0.19		0.19		1.30		0.17				
Ta	0.11	bdl	0.10	bdl	0.12	bdl	0.11	bdl	0.14	Bdl	0.14	bdl	bdl	bdl	bdl
Pb	885	26.7	652	29.7	94.9	68.5	138	68.5	132	68.6	95.1	84.2	13.3	24.2	29.9
Th	0.97	bdl	3.14	bdl	0.36	bdl	0.94	bdl	2.64	Ie	0.09	0.01	0.21	0.06	0.02
U	16.6	0.40	31.2	bdl	0.22	bdl	0.60	bdl	3.95	0.17	0.16	bdl	0.09	0.06	bdl
$^{207}Pb/^{206}Pb$		0.854		0.852		0.854		0.854		0.849		0.857	0.852	0.836	0.938
$^{208}Pb/^{206}Pb$		2.115		2.124		2.113		2.113		2.102		2.114	2.048	2.034	2.511

The REE contents of fluorites MNP-6 and MNP-135 are from Xu et al. (2001). *Represents carbonate mineral measured on fresh mineral grain mounted in a polished epoxy mount with carbonate core exposed. The others were analyzed on bulk rock thin section. WR, whole rock; C, calcite; D, dolomite; bdl, below detection limit; ie, inclusion encountered. $^{207}Pb/^{206}Pb$ is calculated that ratio between determined ^{207}Pb and ^{206}Pb as calibration standard of NIST 610 or 612 multiplies 0.9098 and 0.9073, respectively. $^{208}Pb/^{206}Pb$ is calculated that ratio between determined ^{208}Pb and ^{206}Pb as calibration standard of NIST 610 or 612 multiplies 2.169 and 2.165, respectively (Woodhead and Hergt, 2000). Pb concentrations in carbonate minerals are modeled from ^{208}Pb.

composed of veins of variable size emplaced mostly into syenites, but partially into granites (Fig. 1). These rocks were strongly altered at contacts with the ore veins. The alteration types are similar to those in Daluxiang. The orebodies are divided into three groups according to their characteristic mineral association (Yuan et al., 1995), i.e. (1) pegmatitic bastnäsite-(Ce)–aegirine-augite–fluorite–barite veins (barite veins; >30 cm wide); (2) pegmatitic bastnäsite-(Ce)–fluorite–barite–calcite veins (calcite veins); (3) thread bastnäsite-(Ce)–aegirine-augite–fluorite–barite–calcite veins (thread veins; <30 cm wide). The barite and calcite veins generally extend more than 100 m. They show euhedral–subhedral and pegmatitic texture and ribbon and taxitic structure, and contain 0.5–5 wt.% REE_2O_3. The thread veins are generally about 1 m long and are emplaced around the pegmatitic veins. The K–Ar dates on biotite and arfvedsonite from thread and barite veins suggest an age range of 27.8–31.8 Ma for REE deposition (Yuan et al., 1995). The reserve of REE_2O_3 is estimated to be more than 1.45 million tons. Associated reserves include 0.33 million tons of Pb, 174 tons of Ag, 3.78 million tons of barite and 2.40 million tons of fluorite.

2.3. Bayan Obo

The Bayan Obo REE–Nb–Fe deposit is situated on the northern margin of the Inner Mongolian platform and in the transitional zone between the platform and the Mongolian–Hercynian fold belt (109°59′ E; 41°48′N). Basement strata in the region consist of the Proterozoic Wutai and Bayan Obo Group. The deposit is hosted by the Bayan Obo group, which has been subdivided into nine lithological units, H1–H9 in ascending order (e.g. Bai and Yuan, 1985), and consist predominantly of meta-sandstones and slates, with the exception of the H8 dolomite marble. Interestingly, this unusual unit is the dominant ore-bearing unit. It extends 18 km from east to west, with a width of more than 1 km and occurs as a spindle-shaped stratiform body, widening in the middle and thinning toward the ends (Fig. 1). The H8 horizon includes some bands of biotitized slate and feldspar rock (Yuan et al., 1992). The dolomite marble has a fine- to coarse-grained texture, massive and banded structure, and consists mainly of dolomite and calcite, with feldspar, quartz, Na-tremolite, magnesio-arfvedsonite, phlogopite, apatite, fluorite and barite. The rock also contains REE minerals, such as bastnäsite-(Ce) and monazite-(Ce). Their whole rock Sm–Nd ages are mainly between 1225 and 1656 Ma (Philpotts et al., 1991; Zhang et al., 1994, 2001). The genesis of the dolomite marble is still in dispute; is it sedimentary (Meng, 1982; Chao et al., 1992), or igneous (Liu, 1985; Yuan et al., 1992; Le Bas et al., 1997)? Notably, at least 28 calcite, dolomite and calcite-dolomite carbonatite dykes have been found in this area, ranging from 0.8 to 2.6 m in width (Fig. 1). It is accepted that they are of igneous origin (Le Bas et al., 1992; Tao et al., 1998; Yang et al., 2003). The dates for the carbonatite dykes occur in two clusters, 1223 (whole rock Sm–Nd age; Zhang et al., 1994) to 1416 Ma (zircon U–Pb age; Fan et al., 2006) and 433 (whole rock Rb–Sr age; Bai and Yuan, 1985) to 445 Ma (monazite Pb–Pb age; Ren et al., 1994).

The REE and Nb ores occur throughout the H8 dolomite marble, and Fe ores mainly in the Main, East and West orebodies (Fig. 1). They resemble large lenses or beds, that are orientated parallel to the stratification of the host rock. The boundary between the orebody and its host rocks is gradational. On the basis of textures and structures, three types of Bayan Obo ore can be recognized: disseminated, banded and massive. None are brecciated. Disseminated carbonate-hosted ores range from 3 to 6 wt.% REE_2O_3. Banded ores commonly range from 6 to 12 wt.% REE_2O_3. In contrast, massive ores generally have <3 wt.% REE_2O_3 (Chao et al., 1992). Fluorite, apatite and aegirine are the main gangue

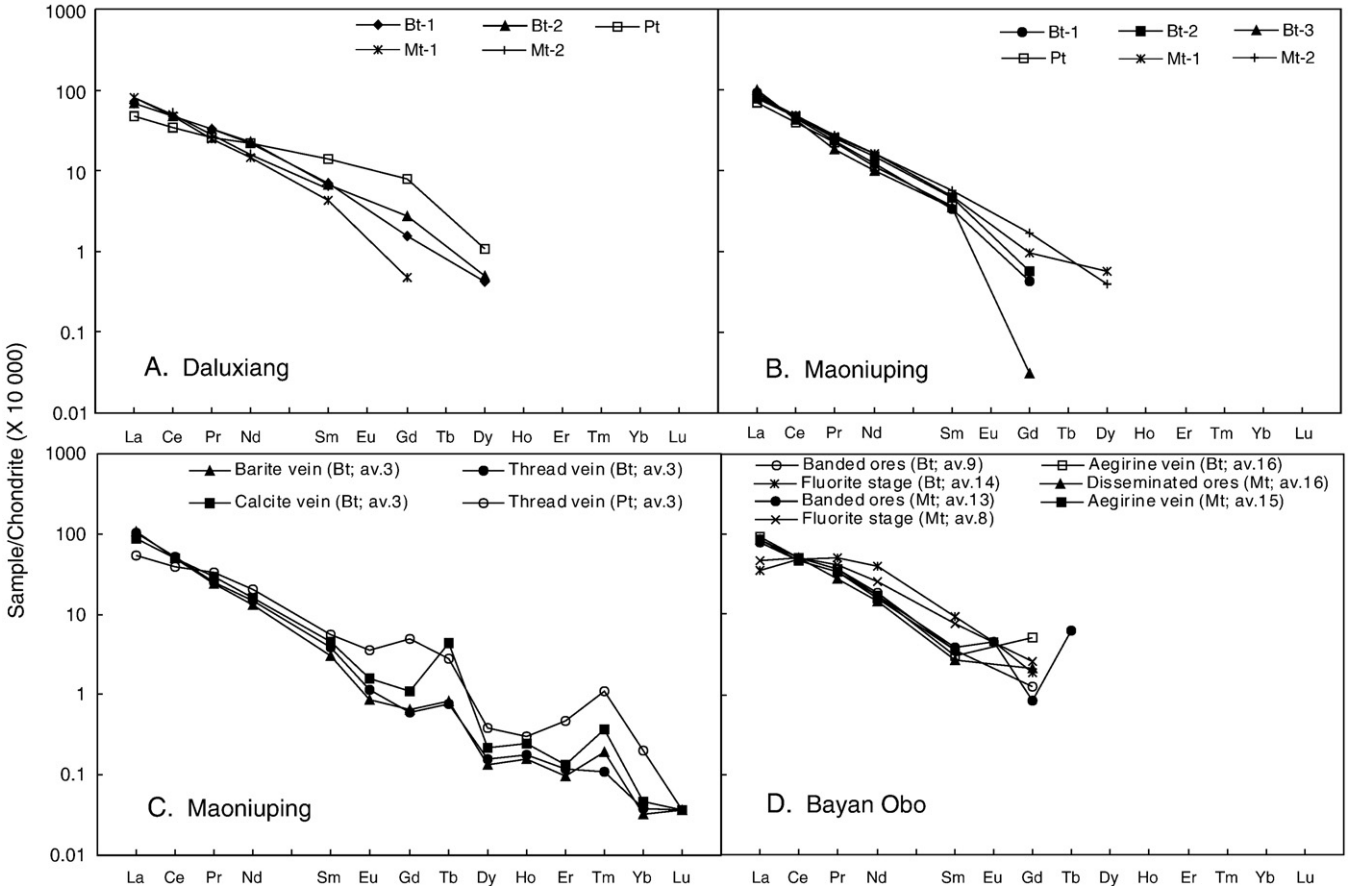

Fig. 3. Chondrite-normalized REE abundances of REE minerals. Bt, bastnäsite-(Ce); Pt, parisite-(Ce); Mt, monazite-(Ce). The data for REE minerals in ore veins from Maoniuping (C) and in H8 dolomite marble (D) are from Yuan et al. (1995) and Smith et al. (2000), respectively. Normalization values are from Sun and McDonough (1989).

minerals. The Bayan Obo deposit has estimated reserves of 600 million tons of iron oxides (Yuan et al., 1992) and in excess of 100 million tons of REE oxides (Ren, 1985). The mineralization age is also in dispute, with suggested ages lying between Mesoproterozoic (Sm–Nd and Th–Pb ages of 1008–1580 Ma; Yuan et al., 1992; Zhang et al., 1994; Liu et al., 2005) and middle Paleozoic (Th–Pb ages of 555–398 Ma; Wang et al., 1994).

Sample BY-810 constitutes coarse-grained (>1 mm; Fig. 2E) dolomite marble and was collected from the north Main orebody, and BY-598 and 599 are fine-grained (<1 mm; Fig. 2F) dolomite marble from Boluotoushan near the northeast East orebody.

3. Analytical methods

The major element compositions of REE minerals and carbonates in the carbonatites were measured on C-coated polished section using a Cameca SX 100 electron microprobe at the Joint Laboratory of Electron Microscopy and Microanalysis, Institute of Geological Sciences, Masaryk University, Brno and Czech Geological Survey using the wavelength-dispersion mode and by wavelength-dispersive EPMA-1600 electron probe at the Institute of Geochemistry, Chinese Academy of Sciences. The following analytical conditions were applied: 15 and 25 kV and a beam current of 10 nA, respectively. The beam was defocused to a 5–10 μm spot size to limit devolatilization of the samples. Mineral standards used for calibration were andradite-Si and Fe (K_α, X-ray line), wollastonite-Ca (K_α), apatite-P (K_α), barite-S (K_α), topaz-F (K_α), ThO_2–Th (M_α), yttrium-aluminium-garnet-Y (K_α), synthetic La–Dy-bearing calcium-aluminium-silicate glasses and La–Dy orthophosphates-La, Ce and Sm (L_α), Pr, Nd, Gd and Dy (L_β) for REE minerals, and dolomite-Mg (K_α), calcite-Ca (K_α), willemite-Mn (K_α), olivine-Fe (K_α) and celestine-Sr (L_α) for carbonate minerals. Data were reduced using the PAP routine (Pouchou and Pichoir, 1984).

Fluorite and carbonatite trace elements were analyzed by solution ICPMS (VG PQ-ExCell) at the University of Hong Kong. Fluorite samples were crushed to 1 mm in size, sieved and washed, then hand-picked for analyses. Fifty mg of the sample powder was dissolved in a Teflon bomb using 1 ml of HF (38%) and 0.5 ml of HNO_3 (68%). The sealed bomb was placed in an electric oven and heated to 190 °C for 12 h. One ml of 1 μg ml^{-1} Rh was added to the cooled solution as the internal standard and the solution was then evaporated. One ml of HNO_3 (68%) was added, evaporated to dryness and followed by a

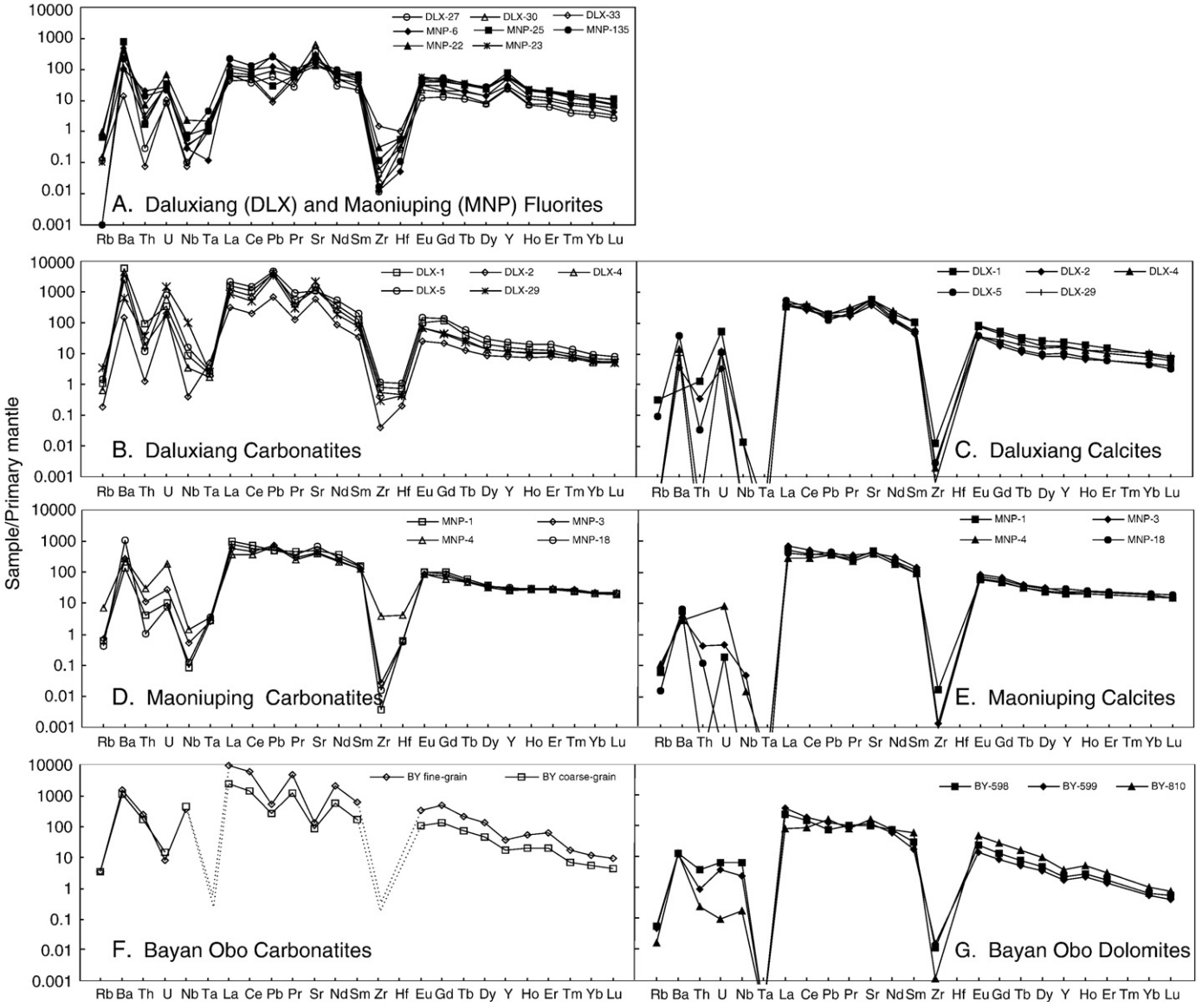

Fig. 4. Primitive mantle-normalized trace element abundances of fluorites (A), carbonatite whole rocks and average carbonate minerals (B–G). The average fine- and coarse-grained dolomite marbles in Bayan Obo are from Xiao et al. (2003). Normalization values are from Sun and McDonough (1989).

second addition of HNO_3 and evaporation to dryness. The final residue was re-dissolved in 8 ml of HNO_3 (40%). The bomb was sealed and heated in an electric oven at 110 °C for 3 h. The final solution was diluted to 100 ml by addition of distilled de-ionized water for ICPMS analysis. Replicate analyses and results from standards indicate that the accuracy of the REE determinations is better than 10%. The details of this procedure are given in Liang et al. (2000).

In situ LA-ICPMS (Agilent 7500S) analyses of carbonate minerals in rock thin sections and mineral grains in polished epoxy mount were performed at the Australian National University. The diameter of the ablation spot varied between 54 and 86 μm. NIST 610 and 612 glasses were used as calibration standard for samples in thin section and polished epoxy mount, respectively. Calculation of elemental concentrations follows Eggins et al. (1997). The element used for the internal standard was Ca, measured as ^{43}Ca and expressed as CaO, which was independently measured by electron microprobe. The detection limits were calculated after Longerich et al. (1996). Analytical precision is ≤5% at the ppm level. In-run signal intensity for indicative trace elements was monitored during analysis to make sure that the laser beam stayed within the phase selected and did not penetrate inclusions.

The LA-ICPMS results include Pb isotopic ratios for masses 206, 207 and 208. The ^{204}Pb cannot be precisely measured because of systemic Hg, and the isobaric interference of ^{204}Hg on ^{204}Pb. Lead concentration was estimated from ^{208}Pb measurements. Isotopic ratios were calculated directly from fractionation factors derived from analysis of the NIST glass standard.

ICPMS sensitivity in dry-plasma (laser) mode is such that the instrument can be tuned for low oxide production, which results in

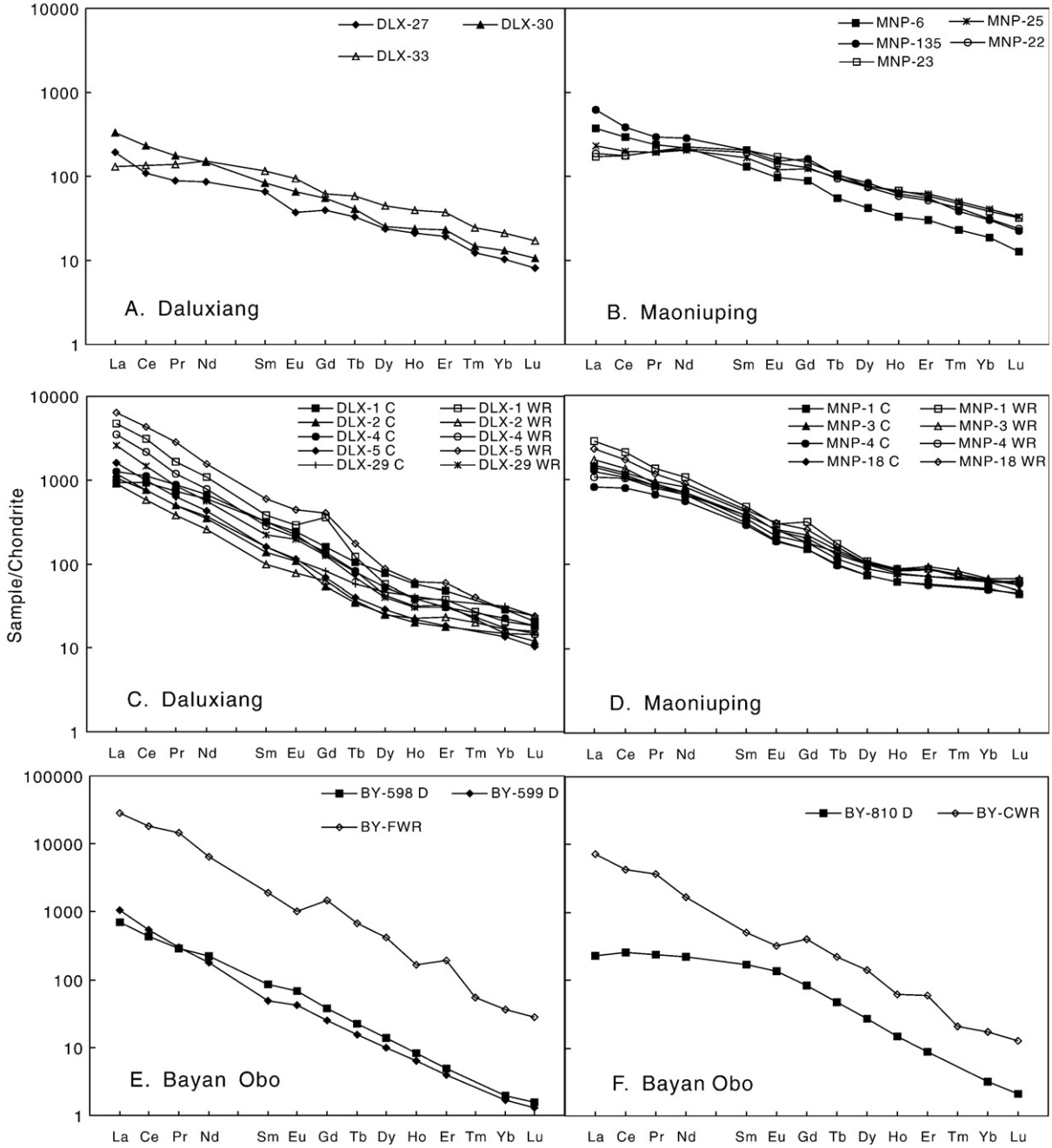

Fig. 5. Chondrite-normalized REE abundances of fluorites (A, B), carbonatites and average carbonate cores (C–F). In A, B the sample DLX-33, MNP-22, 23 are later stage fluorites. In C–F, C=calcite, WR=whole rock, D=dolomite, FWR=fine-grained whole rock, CWR=coarse-grained whole rock. Date sources for fine- and coarse-grained dolomite marbles and normalization values as in Fig. 4.

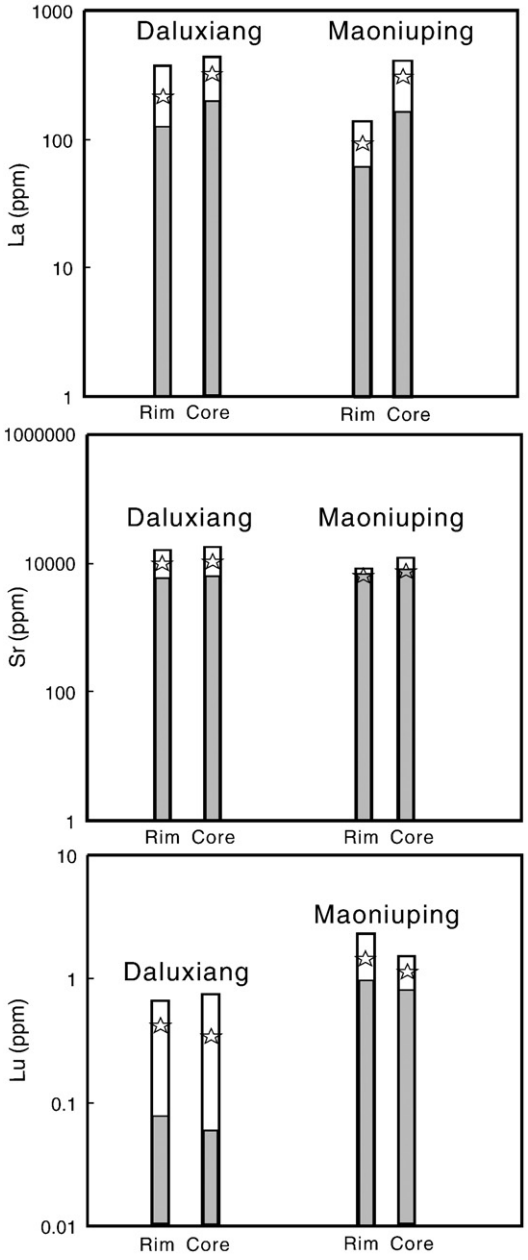

Fig. 6. Comparison of La, Lu and Sr contents between rims and cores of calcites in the Daluxiang and Maoniuping. The white and gray bars and star represent the high, low and average values, respectively. The sample MNP-3 in Maoniuping carbonatites is not included.

very low molecular interferences. The instrument is tuned such that ThO/Th ≤0.5%. All other interferences occur at rates less than this. These conditions are difficult to achieve for wet plasmas, and oxide production for solution ICPMS is commonly a few percent. This fact is important for analysis of REEs in substances with high LREE/HREE ratios like carbonates. LREE oxides interfere with MREEs and HREEs producing spurious positive anomalies. Such analytical anomalies can be seen in some cases in Fig. 5, particularly Gd. Mass 157 suffers oxide interference from Pr mass 141. Other Gd masses are compromised by oxide interferences from La, Ce and Nd. No attempt has been made to correct these interferences.

4. Results

The major element compositions of REE minerals and carbonates analyzed by electron microprobe are given in Tables 1 and 2. Results of the solution ICPMS and LA-ICPMS analyses of fluorites, carbonatites and average carbonate minerals are listed in Table 3. The complete data of carbonate minerals analyzed by LA-ICPMS are shown in Table A online. Note whole rocks were analyzed for Hf and Tm but the carbonate minerals were not.

4.1. REE minerals

The variation of the relative REE abundances in bastnäsite-(Ce), parisite-(Ce) and monazite-(Ce) in carbonatites are shown as chondrite-normalized plots in Fig. 3. Although the parisite-(Ce) has lower La–Nd abundances than bastnäsite-(Ce) and monazite-(Ce), they show a similar enrichment in La relative to Nd. The REE minerals in Daluxiang carbonatites have higher FeO, CaO, Pr_2O_3–Dy_2O_3 and lower La_2O_3, ThO_2 contents than those from Maoniuping. The monazite-(Ce) from carbonatites from the Daluxiang and Maoniuping has higher La_2O_3 and Ce_2O_3 and lower ThO_2 contents than those from Kola, Mountain Pass and Kizilçaören (e.g. Wall and Zaitsev, 2004). Note that the REE compositions and patterns of REE minerals in Maoniuping carbonatites are similar to those in the barite, calcite and thread vein-hosted ores, whereas the REE minerals in Bayan Obo H8 dolomite marbles show variable chondrite normalized $(La/Nd)_N$ ratios from disseminated, banded, and aegirine-hosted to fluorite stage ores.

4.2. Fluorite

The fluorites associated with REE mineralization are enriched in all analyzed elements except Rb, Th, Nb, Zr and Hf on mantle-normalized abundance diagrams (Fig. 4A) and show peaks for Ba, U, La, Sr and Y. The fluorites in Daluxiang have higher Sr contents than those from Maoniuping. They do not have obvious Ce and Eu anomalies, and show similar LREE enriched patterns (Fig. 5A and B). This feature does not correlate with their color or paragenetic settings. The later stage the fluorites in the two deposits show similar depletion of La relative to Nd.

4.3. Carbonate minerals and carbonatites

Calcite is the only carbonate mineral in the Daluxiang and Maoniuping carbonatites. In contrast, the major carbonate mineral at the Bayan Obo H8 samples is dolomite. The Sr contents in Daluxiang calcites are very high. The general geochemical features of the bulk rocks from the three locations are that they show high concentrations of Ba, Pb, Sr and LREEs and a relative depletion in Rb, Ta, Zr and Hf (Fig. 4). The three localities differ in that the Daluxiang and Maoniuping carbonatites are outside of the REE orebodies and have negative Nb anomalies, and the

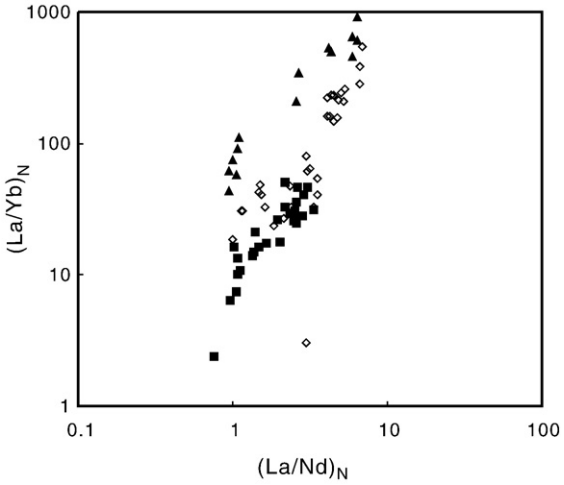

Fig. 7. A plot of $(La/Yb)_N$ vs. $(La/Nd)_N$ for carbonatites and carbonate minerals. ◊, Daluxiang; ■, Maoniuping; ▲, Bayan Obo.

Daluxiang carbonatites have positive Pb and Sr anomalies, whereas the Bayan Obo H8 dolomite marbles are much more enriched in Th, Nb and LREEs than the others, and have negative Pb and Sr anomalies. The carbonate minerals in all three deposits have lower Th, U, Nb, Ta and Zr contents than their corresponding whole rocks. In contrast, the dolomites from Bayan Obo have higher U, Th, Nb and lower Sr and Y concentrations than the calcites from Daluxiang and Maoniuping.

Focusing on the REEs, the chondrite-normalized REE patterns for the whole rocks are strongly LREE enriched without obvious Ce or Eu anomalies (Fig. 5), a feature typical of carbonatites worldwide (Nelson et al., 1988; Woolley and Kempe, 1989; Hornig-Kjarsgaard, 1998; and references therein). The carbonate cores show similar REE patterns to the whole rocks (except for sample BY-810), and REE contents gradually increase from 1–80 times the chondritic value for Lu to 150–2500 times chondrite for La (Fig. 5). The calcites in Daluxiang and Maoniuping carbonatites have high REE contents, close to their whole rocks. Systematic differences between core and rim compositions have been found in some analyzed minerals (Table A online). Except for the sample MNP-3, LREE (e.g. La) contents gradually decrease from core to rim (Fig. 6), suggesting that LREEs have been removed into a fluid that separated from the carbonatite magmas. Bühn and Rankin (1999) suggested that the carbonatite-expelled fluids were characterized by low viscosity and were rich in alkali and volatile. They can concentrate huge amounts of REEs and Sr because of their high H_2O–CO_2–Cl–F contents. Additionally, in some cases the grain core has higher Sr, but lower HREE (e.g. Lu) contents than the corresponding rim (Fig. 6). These carbonate minerals are distinct in the ratio-ratio plot of Fig. 7 designed to indicate the steepness (*y* axis) and curvature (*x*-axis) of the REE plots. The Bayan Obo samples have steeper slopes than Daluxiang and Maoniuping, and REE contents are almost 100 times lower than the whole-rock data. The coarse-grained sample BY-810 has a relatively low $(La/Nd)_N$ ratio.

Reconnaissance LA-ICPMS $^{208}Pb/^{206}Pb$ and $^{207}Pb/^{206}Pb$ ratios are plotted in Fig. 8. The contribution of radiogenic Pb is assumed to be negligible given that the carbonate minerals contain tens of ppm Pb, and have U and Th that are below the detection limits of the LA-ICPMS (Table 3). Two sigma (2σ) error bars are included. The calcites in Daluxiang and Maoniuping carbonatites have similar Pb isotopic compositions and fall between the mantle end-members EM1 and EM2. The Pb isotopic data of the Maoniuping calcites are consistent with the whole rock analyses of Xu et al. (2004). Their initial Sr (0.7061–0.7069) and Nd isotopes (ε_{Nd} = −5.6 to −3.4) (Xu et al., 2003a) also plot between EM1 and EM2. The initial Sr isotopes (0.7078–0.7080; Xu et al., unpublished) of calcites in Daluxiang carbonatites are close to the EM2, however, their ε_{Nd} (−18.9 to −6.4; Hou et al., 2006) show a large range. The carbonatites in Daluxiang have markedly positive Pb anomalies in Fig. 4B, different to those from Maoniuping, suggesting that the former was a contamination by continental crust. Their calcites do not show positive Pb anomalies (Fig. 4C) and have consistent $^{207}Pb/^{206}Pb$ and $^{208}Pb/^{206}Pb$ ratios with those in Maoniuping, which suggests that the Pb isotopes in calcites may be an ideal tool to identify the mantle characteristics of carbonatites in the Panxi region. They track a line between EM1 and EM2 and are distinct from the East African carbonatites (EAC), which formed in a rifting environment and were interpreted as mixing between HIMU and EM1 in Pb vs Pb and Sr vs Pb isotopic diagrams (Fig. 8). The latter also defines the similar trend called East African Carbonatite Line (EACL) on ε_{Nd}–$^{87}Sr/^{86}Sr$ diagram. In contrast, the Daluxiang and Maoniuping carbonatites have higher $^{87}Sr/^{86}Sr$, $^{207}Pb/^{206}Pb$ and $^{208}Pb/^{206}Pb$ ratios. The reported age for carbonatites in Maoniuping is 31.7 Ma (Pu, 2001), subsequent to the collision between the Indian and Asian continents at 45–65 Ma in south Tibet, which

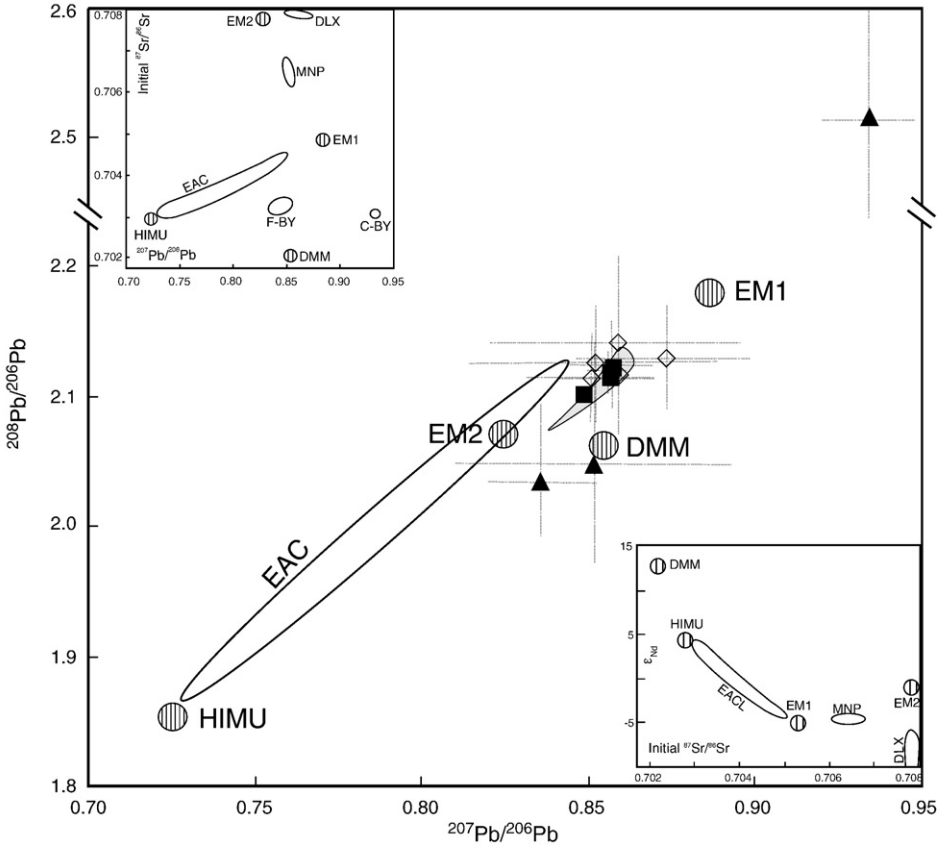

Fig. 8. $^{208}Pb/^{206}Pb$ vs. $^{207}Pb/^{206}Pb$ diagram for in situ analyses of average carbonate minerals. Symbols as in Fig. 7; EAC, East African carbonatites (Bell and Tilton, 2001); EACL, East African Carbonatite Line (Bell and Blenkinsop, 1987); DLX, Daluxiang; MNP, Maoniuping; BY, Bayan Obo; F, fine grain; C, coarse grain. The grey range represents Maoniuping carbonatites (Xu et al., 2004). Sr and Nd isotopes for Daluxiang, Maoniuping and Bayan Obo carbonatites are from Hou et al. (2006), Xu et al. (2003a) and Le Bas et al. (1997), respectively. DMM, HIMU, EM1, EM2 are the mantle end-member compositions from Hart et al. (1992). The error bars are in-run precision (2σ, standard error).

resulted in the formation of the collision zone along the eastern margin of the Tibetan plateau (Yin and Harrison, 2000). The carbonatite sources in the Panxi region may involve recycling of a few subducted pelagic and terrigenous sediments (<5%) into the deep mantle, as modeled by Hou et al. (2006).

The Pb isotopes for three Bayan Obo samples show different compositions. The fine-grained dolomite has low thorogenic Pb. However, the coarse-grained sample has high $^{207}Pb/^{206}Pb$ and $^{208}Pb/^{206}Pb$ ratios and lies beyond known mantle compositions. Its origin may involve mixing with fluids derived from lower crust and characterized by low $^{87}Sr/^{86}Sr$, high $^{207}Pb/^{206}Pb$ and $^{208}Pb/^{206}Pb$ ratios (Zartman and Doe, 1981).

5. Discussion

The paragenesis of the Bayan Obo deposit is complex with multiple stages of deposition (e.g. Chao et al., 1992). Various origins have been proposed with models involving fluids derived from carbonatite or alkaline magmatism (Yuan et al., 1992; Campbell and Henderson, 1997; Smith and Henderson, 2000; Smith, 2007), subduction (Wang et al., 1994), or A-type granite magmatism (Chao et al., 1997). The genesis of the H8 dolomite marble, which hosts the vast majority of ores, is still being disputed. Because of their relative simplicity we first discuss the genesis of Daluxiang and Maoniuping deposits as they are representative deposits in the REE mineralization belt in the Panxi region.

It is generally agreed that the Daluxiang and Maoniuping carbonatites are of igneous origin. Their $\delta^{13}C_{PDB}$ and $\delta^{18}O_{SMOW}$ values range from −6.6 to −7.0‰, 6.4 to 7.4‰, and −5.9 to −8.5‰, 6.7 to 10.5‰ (Xu et al., 2003b; Hou et al., 2006), respectively, which are mostly within the primary, mantle-derived carbonatites on the $\delta^{18}O$–$\delta^{13}C$ diagram as defined by Keller and Hoefs (1995). The calcites in carbonatites analyzed by in situ LA-ICPMS are characterized by high REE and Sr contents. Their Pb isotopic compositions also show EM1–EM2 enriched mantle signatures.

The following evidence suggests that the REE deposits in the Panxi region are associated with the fluids derived from carbonatite magmatism: (1) the ages for the ore mineralization and the carbonatites are similar (27.8–31.8 Ma and 31.7 Ma in Maoniuping; Yuan et al., 1995; Pu, 2001); (2) REE minerals in Maoniuping carbonatites have similar REE abundances and patterns to those in ore veins from the three groups of orebodies (Fig. 3); (3) fluorite is one of main gangue minerals associated with REE deposition. Williams-Jones et al. (2000) suggested that the occurrence of fluorite was an excellent exploration guide for REE-fluorocarbonante mineralization in environments where alkaline igneous rocks or carbonatites have been emplaced. Fluid inclusion studies showed the fluorites formed from high temperature and salinity fluids (249–760 °C for Daluxiang; 204–556 °C, 5.7–21 wt.% NaCl for Maoniuping; Niu et al., 1997; Pu, 2001). Fluid-melt inclusions were found in the fluorites (Niu et al., 1997; Pu, 2001). Bastnäsite-(Ce) deposition occurred over a large range of temperature and at high salinities (274–430 °C for Daluxiang; 116–196 °C, 12–20 wt.% NaCl for Maoniuping; Yuan et al., 1995; Pu, 2001). The fluids associated with mineralization are interpreted to have been of the orthomagmatic origin, and the contribution from meteoric or ground water is negligible. According to data presented by Wood (1990), F^- and CO^{2-}_3 form the strongest complexes with REEs. The compositions of carbonatites and their minerals (such as fluorite, apatite, amphibole and mica), and unusually alkalic carbonatite lava flows at Oldoinyo Lengai, which contain up to 15% F+Cl, showing that fluorine plays an important role in carbonatite magmas (Jago and Gittins, 1991). Moreover, a major proportion of F partitioned preferentially into the fluids that were expelled from a carbonatite magma (Bühn and Rankin, 1999); (4) The more interesting features to emerge from Figs. 4 and 5 are that the fluorites in Daluxiang show higher Sr and lower HREE contents than those from Maoniuping, which is consistent with the differences found in the carbonatites and calcites. The ore-forming and later-stage fluorites in Maoniuping also have similar Sr and Nd isotope compositions to the carbonatites (Xu et al., 2003b). This implies that the fluorite deposition, probably including the REE minerals, involved the carbonatite-derived fluids.

It is noted that the ore veins are outside of the carbonatite areas. Most occur in syenites but some are found in granites. Fluoritization, carbonatization and bastnäsitization are common at the contact between the ore-veins and country rocks. The REE minerals in carbonatites are quite minor, and most of REEs are concentrated in calcite (Fig. 5). It is clear that the REE compositions of the Daluxiang and Maoniuping sampled rocks do not represent melts because the calcites have the same REE concentrations to their associated whole rocks. These carbonatite compositions can only represent magmas if the carbonate mineral/melt partition coefficients (*Ds*) of all REEs are ~1, which is unlikely. Although quantitative *Ds* in carbonate mineral/carbonatite melt have not yet been determined, it is almost certain that the *Ds* for REEs are much less than 1 (e.g. Bühn et al., 2001). Furthermore, their $CaCO_3$ content (~90%) is too high to represent a calciocarbonatite magma generated after metasomatism of wall rock lherzolite, which produce carbonate liquids containing no more than 75–87% $CaCO_3$ (Dalton and Wood, 1993). The carbonatites may be interpreted to be calcite-rich cumulates (e.g. Woolley and Church, 2005; Xu et al., 2007). The crystallization and accumulation of calcite would result in the REE enrichment in the carbonatite-expelled fluids. In addition, fluorite, because of its low solubility, was deposited immediately on the interaction between migrating REE-fluoride-enriched fluids and the syenite–granite country rocks. This produced a sharp drop in the activity of F^-, which destabilized the REE fluoride complexes and caused deposition of REE minerals. The fact that the syenites and granites were replaced by bastnäsite-(Ce) and fluorite provides evidence for this interpretation. The LREE depletion in the later fluorites also results from the mineralization processes.

The H8 dolomite marble of the Bayan Obo is unlikely to be of sedimentary origin, because (1) the dolomite marbles show intrusive contact with country rocks (Liu, 1985). The metamorphism is present at the contact. Moreover, they display a flow structure and contain xenoliths of country rocks (Liu, 1985); (2) both the coarse- and fine-grained dolomite marbles contain lower $^{87}Sr/^{86}Sr$ ratios of 0.7024–0.7061 than the limestones from the strata H1–H7 that are clearly of sedimentary origin (0.720–0.726; Liu, 1985; Le Bas et al., 1997). If the H8 dolomite marble was a re-crystallization product of a sedimentary dolostone, which was replaced by the fluids derived from carbonatite or granite magmatism, it would have higher Sr isotopic compositions than the latter. Some dolomite marbles show lower initial $^{87}Sr/^{86}Sr$ ratios (~0.7030) relative to the adjacent carbonatite dykes (0.7064–0.7089; Le Bas et al., 1992; Bai and Yuan, 1996) and granites (0.7071–0.7088; Yang et al., 2000b). In addition, our dolomite samples also have much higher Sr, REE and MnO contents than the sedimentary limestones (129–165 ppm, 20 ppm and <0.1% for Sr, total REEs and MnO, respectively; Le Bas et al., 1997; Yang and Le Bas, 2004) and Veizer's average dolostone (40 ppm, 25 ppm and 0.2% for Sr, total REEs and MnO, respectively; Veizer et al., 1992). It is well known that carbonatites tend to be very enriched in Sr (e.g. Nelson et al., 1988; Woolley and Kempe, 1989; Hornig-Kjarsgaard, 1998) and our data show that most of Sr in the Bayan Obo dolomite marbles are held in the dolomites (Fig. 4).

Many studies of the Bayan Obo REE–Nb–Fe deposit have suggested that the REE mineralization was episodic, with major episodes in the Mesoproterozoic and Caledonian. Some carbonatite dykes in the north of the East orebody (Fig. 1) have similar compositions of REE phases (Yang et al., 2000a) and age to the Mesoproterozoic H8 dolomite marbles. This implies that the Mesoproterozoic REE mineralization in Bayan Obo is related to carbonatite magma activity. In addition, the fine- and coarse-grained dolomites show different geochemical compositions, and the former has lower FeO, higher LREE and Nb contents. Their $^{207}Pb/^{206}Pb$ and $^{208}Pb/^{206}Pb$ ratios are also lower and close to the mantle compositions. The fine-grained dolomite may be a re-crystallization product (Le Bas et al., 1997), which was replenished by external

REE-, Nb- and even Sr-rich fluids, because the dolomite is characterized by high Sr content. Similarly, different stage apatite is also very rich in Sr and appears to be carbonatite associated (Campbell and Henderson, 1997). An alternative source for the external fluids is required and the adjacent carbonatite dykes are an obvious candidate. This interpretation is consistent with the previous studies of fluid inclusions (Smith and Henderson, 2000). Whole rock Rb–Sr and monazite Th–Pb ages from the carbonatite dykes suggested that they were remobilized during Caledonian orogeny (Bai and Yuan, 1985; Ren et al., 1994). Moreover, the fine-grained dolomites have slightly lower and parallel REE concentrations relative to calcites from the Daluxiang and Maoniuping carbonatites. This indicates that the carbonatite-derived fluids related to mineralization in Bayan Obo may concentrate rather higher REE compositions than those in Daluxiang and Maoniuping deposits, because dolomite has a lower affinity to REEs than calcite ($D_{\text{dolomite/calcite}}$ for La–Lu range from 0.16 to 0.23; Dawson and Hinton, 2003). This may explain why Bayan Obo is a world-class deposit.

Since fluorite is not only strikingly abundant at Bayan Obo, but petrographically associated with REE and Nb minerals as well, it is very reasonable to infer F-complexes dominated the REE-, and even Nb-species in the ore-forming fluids. Experimentally determined biotite/granitic melt *Ds* for F range from 1.5 to 7.2 (Icenhower and London, 1997). Amphibole and biotite associated with Nb mineralization are both enriched in fluorine (1.25–3.36 and 8.10%, respectively; Smith, 2007), suggesting that high F^- activities may be critical for the formation of Nb mineralization. Our comparative study of the Bayan Obo deposit with the Daluxiang and Maoniuping deposits, suggests that a similar deposition mechanism is required for all three deposits. The F-rich and carbonatite-derived fluids, with high REEs and Nb, interacted with the H8 dolomite marbles, which resulted in complex metasomatic phenomena displayed by the ore and gangue mineral paragenesis in Bayan Obo (Smith et al., 1999).

6. Conclusions

At Daluxiang and Maoniuping, the calcites from carbonatites are characterized by high Sr, REE concentrations and LREE enriched patterns that are parallel to the corresponding whole rocks. These rocks may be calcite-rich cumulates. The crystallization and accumulation of the calcites produced a strong REE enrichment in the carbonatite-derived fluids. It is noted that the calcites and their whole rocks in Daluxiang have lower HREE and higher Sr contents than those from Maoniuping. Similar differences are also seen in the chemical compositions of fluorite, which is closely associated with the REE mineralization. This supports a model for the genesis of the Daluxiang and Maoniuping ores involving carbonatite-related fluids interacting with country rocks, which resulted in fluoritization, carbonatization and bastnäsitization developed at contacts of the country rocks with ore veins. The high MnO, Sr and REE contents in dolomites from the H8 dolomite marbles in Bayan Obo suggest an igneous origin. However, the fine-grained dolomite has higher LREEs and Nb, and lower FeO and $^{207}Pb/^{206}Pb$ and $^{208}Pb/^{206}Pb$ ratios than the coarse-grained dolomite. These data indicate that the fine-grained dolomite may be a re-crystallization product, which was replenished by external REE- and Nb-rich fluids derived from the adjacent carbonatite dykes. This interpretation is consistent with a carbonatite-derived, metasomatic/hydrothermal model with H8 dolomite marbles acting as host for REE and Nb ore formation, similar to the Daluxiang and Maoniuping deposits.

Acknowledgments

We thank Dr. Mei-Fu Zhou for supporting trace element analysis and Prof. Tiegeng Liu for providing the Bayan Obo carbonatite thin sections. Frances Wall and an anonymous reviewer are thanked for reviewing and improving the manuscript. Editorial comments by Nelson Eby also improve sections of this manuscript. This research was financially supported by the Chinese National Science Foundation (No. 40773021) and the Chinese '973' Project (No. 2006CB403508) and President Fund of Chinese Academy of Sciences to C. Xu.

Appendix A. Supplementary data

Supplementary data associated with this article can be found, in the online version, at doi:10.1016/j.lithos.2008.06.005.

References

Andrade, F.R.D., Möller, P., Luders, V., Dulski, P., Gilg, H.A., 1999. Hydrothermal rare earth elements mineralization in the Barra do Itapirapuã carbonatite, southern Brazil: behavior of selected trace elements and stable isotopes C, O. Chemical Geology 155, 91–113.

Bell, K., Blenkinsop, J., 1987. Nd and Sr isotopic compositions of East African carbonatites: implications for mantle heterogeneity. Geology 15, 99–102.

Bühn, B., Rankin, A.H., 1999. Composition of natural, volatile-rich Na–Ca–REE–Sr carbonatitic fluids trapped in fluid inclusions. Geochimica et Cosmochimica Acta 63, 3781–3797.

Bai, G., Yuan, Z.X., 1985. Carbonatites and related mineral resources. Bulletin of Institute of Mineral Deposits, vol. 13. Chinese Academy of Geological Sciences, pp. 107–140 (in Chinese).

Bai, G., Yuan, Z.X., 1996. Demonstration on the Geological Feature and Genesis of the Baynan Obo Deposit. Geological Publishing House, Beijing. (in Chinese).

Bell, K., Tilton, G.R., 2001. Nd, Pb, and Sr isotopic compositions of East African cabonatites: evidence for mantle mixing and plume inhomogeneity. Journal of Petrology 42, 1927–1945.

B ü hn, B., Wall, F., Le Bas, M.J., 2001. Rare-earth element systematics of carbonatitc fluorapatites, and their significance for carbonatite magma evolution. Contributions to Mineralogy and Petrology 141, 572–591.

Campbell, L.S., Henderson, P., 1997. Apatite paragenesis in the Bayan Obo REE–Nb–Fe ore deposit, Inner Mongolia, China. Lithos 42, 89–103.

Chao, E.C.T., Back, J.M., Minkin, J.A., Ren, Y.C., 1992. Host-rock controlled epigenetic, hydrothermal metasomatic origin of the Bayan Obo REE–Fe–Nb ore deposit, Inner Mongolia, P.R.C. Applied Geochemistry 7, 443–458.

Chao, E.C.T., Back, J.M., Minkin, J.A., Ren, Y.C., 1997. The sedimentary carbonate giant Bayan Obo REE–Fe–Nb ore deposit of Inner Mongolia, China: a cornerstone example for giant polymetallic ore deposit of hydrothermal origin. US Geological Survey Bulletin 2143, 1–65.

Dalton, J.A., Wood, B.J., 1993. The compositions of primary carbonate melts and their evolution throng wallrock reaction in the mantle. Earth and Planetary Science Letters 119, 511–525.

Dawson, J.B., Hinton, R.W., 2003. Trace-element content and partitioning in calcite, dolomite and apatite in carbonatite, Phalaborwa, South Africa. Mineralogy and Petrology 67, 921–930.

Eggins, S.M., Woodhead, J.D., Kinsley, L.P.J., Mortimer, G.E., Sylvester, P., McCulloch, M.T., Hergt, J.M., Handler, M.R., 1997. A simple method for the precise determination of ≥40 trace elements in geological samples by ICPMS using enriched isotope internal standardization. Chemical Geology 134, 311–326.

Fan, H.R., Hu, F.F., Chen, F.K., Yang, K.F., Wang, K.Y., 2006. Intrusive age of carbonatite dyke from Bayan Obo REE–Nb–Fe deposit. Inner Mongolia: with answers to comment of Dr. Le Bas. Acta Petrologica Sinica 22, 519–520 (in Chinese with English abstract).

Hart, S.R., Hauri, E.H., Oschmann, L.A., Whitehead, J.A., 1992. Mantle plumes and entrainment: isotopic evidence. Science 256, 517–520.

Hornig-Kjarsgaard, I., 1998. Rare earth elements in sövitic carbonatites and their mineral phases. Journal of Petrology 39, 2105–2121.

Hou, Z.Q., Tian, S.H., Yuan, Z.X., Xie, Y.L., Yin, S.P., Yi, L.S., Fei, H.C., Yang, Z.M., 2006. The Himalayan collision zone carbonatites in western Sichuan, SW China: petrogenesis, mantle source and tectonic implication. Earth and Planetary Science Letters 244, 234–250.

Icenhower, J.P., London, D., 1997. Partitioning of fluorine and chlorine between biotite and granitic melt: experimental calibration at 200 MPa H_2O. Contributions to Mineralogy and Petrology 127, 17–29.

Jago, B.C., Gittins, J., 1991. The role of fluorine in carbonatite magma evolution. Nature 349, 56–58.

Keller, J., Hoefs, J., 1995. Stable isotope characteristics of recent natrocarbonatites from Oldoinyo Lengai. In: Bell, K., Keller, J. (Eds.), Carbonatites Volcanism: Oldoinyo Lengai and Petrogenesis of Natrocarbonatites. LAVCEI Proceeding in Volcanology. Springer-Verlag, Berlin, pp. 113–123.

Le Bas, M.J., Keller, J., Tao, K.J., Wall, F., Williams, C.T., Zhang, P.S., 1992. Carbonatite dykes at Bayan Obo, Inner Mongolia, China. Mineralogy and Petrology 46, 195–228.

Le Bas, M.J., Spiro, B., Yang, X.M., 1997. Oxygen, carbon and strontium isotope study of the carbonatitic dolomite host of the Bayan Obo Fe–Nb–REE deposit, Inner Mongolia, China. Mineralogical Magazine 61, 531–541.

Li, X.Y., 2005. Geological characteristics of Daluxiang REE deposit in Dechang County, Sichuan Province. Mineral Deposits 24, 151–160 (in Chinese with English abstract).

Liang, Q., Hu, J., Gregoire, D.C., 2000. Determination of trace elements in granites by inductively coupled plasma mass spectrometry. Talanta 51, 507–513.

Liu, T.G., 1985. Geological and geochemical character of Bayan Obo dolomite marble. Acta Petrologica Sinica 1, 15–28 (in Chinese with English abstract).

Liu, Y.L., Chen, J.F., Li, H.M., Qian, H., Xiao, G.W., Zhang, T.R., 2005. Single-grain U–Th–Pb–Sm–Nd dating of monazite from dolomite type ore of the Bayan Obo deposit. Acta Petrologica Sinica 21, 881–888 (in Chinese with English abstract).
Longerich, H.P., Jackson, S.E., Gunter, D., 1996. Laser ablation inductively coupled plasma mass spectrometric transient signal data acquisition and analyze concentration calculation. Journal of Analytical Atomic Spectrometry 11, 899–904.
Mariano, A.N., 1989. Nature of economic mineralization in carbonatites and related rocks. In: Bell, K. (Ed.), Carbonatites: Genesis and Evolution. Unwin Hyman, London, pp. 149–175.
Meng, Q.R., 1982. The genesis of the host rock dolomite of the Bayan Obo iron ore deposit and analysis of its sedimentary environment. Geological Review 28, 481–489 (in Chinese with English abstract).
Nelson, D.R., Chivas, A.R., Chappell, B.W., McCulloch, M.T., 1988. Geochemical and isotopic systematics in carbonatites and implications for the evolution of ocean-island sources. Geochimica et Cosmochimica Acta 52, 1–17.
Niu, H.C., Shan, Q., Chen, P.R., 1997. Natures of fluids in magmatic-hydrothermal transitional stage-exemplified by Maoniuping deposit, Sichuan, China. Journal of Nanjing University 33, 21–27 (in Chinese with English abstract).
Philpotts, J., Tatsomoto, M., Li, X.F., Wang, K., 1991. Some Nd and Sr isotopic systematics from the REE-enriched deposit at Bayan Obo, China. Chemical Geology 90, 177–178.
Pouchou, J.L., Pichoir, F., 1984. A new model for quantitative analysis. I. Application to the analysis of homogeneous samples. La Récherche Aerosp 3, 13–38.
Pu, G.P., 1988. Discovery of an alkalic pegmatite-carbonatite complex zone in Maoniuping, southwestern Sichuan Province. Geology Review 34, 88–92 (in Chinese with English abstract).
Pu, G.P., 2001. The evolution history of REE mineralization and major features of Himalayan REE deposit in Panzhihua–Xichang area, Sichuan. In: Chen, Y.C., Wang, D.H. (Eds.), Study on Himalayan Endognic Mineralization. Geological Publishing House, Beijing, pp. 104–116 (in Chinese).
Ren, J., 1985. A brief account on the geology of rare earth mineralization in China. In: Xu, G., Xiao, J. (Eds.), New Frontiers in Rare Earth Science and Applications, vol. 1. Science Press, Beijing, pp. 39–41 (in Chinese).
Ren, Y., Zhan, Y., Zhan, Z., 1994. Study on the heat events of ore forming Bayan Obo deposit. Acta Geoscientia Sinica 1–2, 95–101 (in Chinese with English abstract).
Smith, M.P., 2007. Metasomatic silicate chemistry at the Bayan Obo Fe-REE–Nb deposit, Inner Mongolia, China: contrasting chemistry and evolution of fenitising and mineralising fluids. Lithos 93, 126–148.
Smith, M.P., Henderson, P., 2000. Preliminary fluid inclusion constraints on mineralising fluid evolution in the Bayan Obo Fe-REE–Nb deposit, Inner Mongolia, China. Economic Geology 95, 1371–1388.
Smith, M.P., Henderson, P., Zhang, P.S., 1999. Reaction relationships in the Bayan Obo Fe–REE–Nb deposit Inner Mongolia, China: implications for the relative stability of rare-earth element phosphates and fluorocarbonates. Contributions to Mineralogy and Petrology 134, 294–310.
Smith, M.P., Henderson, P., Campbell, L.S., 2000. Fractionation of the REE during hydrothermal processes: constraints from the Bayan Obo Fe-REE–Nb deposit, Inner Mongolia, China. Geochimica et Cosmochimica Acta 64, 3141–3160.
Sun, S.S., McDonough, W.F., 1989. Chemical and isotopic systematics of oceanic basalt: implications for mantle compositions and processes. In: Saunders, A.D., Norry, M.J. (Eds.), Magmatism in the Ocean Basins. Special Publication, vol. 42. The Geological Society, pp. 313–345.
Tao, K., Yang, Z., Zhang, Z., Wang, W., 1998. Systematic geological investigation on carbonatite dykes in Bayan Obo, Inner Mongolia, China. Scientia Geologica Sinica 33, 73–83 (in Chinese with English abstract).
Veizer, J., Plumb, K.A., Clayton, R.N., Hinton, R.W., Grotzinger, J.P., 1992. Geochemistry of Precambrian carbonates: V. Late Paleoproterozoic seawater. Geochimica et Cosmochimica Acta 56, 2487–2501.
Wall, F., Mariano, A.N., 1996. Rare earth minerals in carbonatites: a discussion centred in the Kangankunde carbonatite, Malawi. In: Jones, A.P., Wall, F., Williams, C.T. (Eds.), Rare Earth Minerals: Chemistry, Origin and Ore Deposits. The Mineralogical Society Series 7. Chapman and Hall, London, pp. 193–225.
Wall, F., Zaitsev, A.N., 2004. Rare earth minerals in Kola carbonatites. In: Wall, F., Zaitsev, A.N. (Eds.), Phoscorites and Carbonatites from Mantle to Mine: the Key Example of the Kola Alkaline Province. The Mineralogical Society Series, 10. Mineralogical Society, London, pp. 341–373.
Wang, J., Tasumoto, M., Li, X., Premo, W.R., Chao, E.C.T., 1994. A precise 232Th–208Pb chronology of fine-grained monazite: age of the Bayan Obo REE–Fe–Nb ore deposit, China. Geochimica et Cosmochimica Acta 58, 3155–3169.
Williams-Jones, A.E., Samson, I.M., Olivo, G.R., 2000. The genesis of hydrothermal fluorite-REE deposits in the Gallinas Mountains, New Mexico. Economic Geology 95, 327–342.
Wood, S.A., 1990. The aqueous geochemistry of the rare-earth elements and yttrium, 1. Review of available low-temperature data for inorganic complexes and the inorganic REE speciation of nature waters. Chemical Geology 82, 159–186.
Woodhead, J.D., Hergt, J.M., 2000. Pb-isotope analyses of USGS reference materials. Geostandards 24, 33–38.
Woolley, A.R., Church, A.A., 2005. Extrusive carbonatites: a brief review. Lithos 85, 1–14.
Woolley, A.R., Kempe, D.R.C., 1989. Carbonatites: nomenclature, average chemical composition. In: Bell, K. (Ed.), Carbonatites: Genesis and Evolution. Unwin Hyman, London, pp. 1–14.
Xiao, R.G., Fei, H.C., An, G.Y., Zhang, H.C., Hou, W.R., 2003. Lithology and genesis of dolomite marble in Bayan Obo mine, Inner Mongolia. Geoscience 17, 287–293 (in Chinese with English abstract).
Xu, C., Huang, Z.L., Liu, C.Q., Qi, L., Li, W.B., Guan, T., 2001. Sources and evolution of ore-forming fluids of the Maoniuping rare-earth deposit: evidence from REE geochemistry of fluorites. Geology and Prospecting 37, 24–28 (in Chinese with English abstract).
Xu, C., Huang, Z.L., Liu, C.Q., Qi, L., Li, W.B., Guan, T., 2003a. Geochemistry of carbonatites in Maoniuping REE deposit, Sichuan Province, China. Science in China (D) 46, 246–256.
Xu, C., Huang, Z.L., Liu, C.Q., Qi, L., Li, W.B., Guan, T., 2003b. Indicator of fluorite Sr and Nd isotopes to mantle-derived ore-forming fluids in the Maoniuping REE deposit, Sichuan Province, China. Earth Science 28, 41–46 (in Chinese with English abstract).
Xu, C., Huang, Z.L., Liu, C.Q., Yuan, Z.F., Li, W.B., Guan, T., 2004. Pb isotopic geochemistry of carbonatites in Maoniuping REE deposit, Sichuan Province, China. Acta Petrologica Sinica 20, 495–500 (in Chinese with English abstract).
Xu, C., Campbell, I.H., Allen, C.M., Huang, Z.L., Qi, L., Zhang, H., Zhang, G.S., 2007. Flat rare earth element patterns as an indicator of cumulate processes in the Lesser Qinling carbonatites, China. Lithos 95, 267–278.
Yang, X.M., Le Bas, M.J., 2004. Chemical compositions of carbonate minerals from Bayan Obo, Inner Mongolia, China: implications for petrogenesis. Lithos 72, 97–116.
Yang, X.M., Yang, X.Y., Zhang, P.S., Le Bas, M.J., 2000a. Ba-REE fluocarbonate minerals from a carbonatite dyke at Bayan Obo, Inner Mongolia, North China. Mineralogy and Petrology 70, 221–234.
Yang, X.M., Yang, X.Y., Fan, H.R., Guo, F., Zhang, Z.F., Zhang, P.S., 2000b. Rare earth element geochemistry of the Heicynian granite complex at Bayan Obo, Inner Mongolia, China. Chinese Rare Earths 21, 1–7 (in Chinese with English abstract).
Yang, X.M., Yang, X.Y., Zheng, X.F., Le Bas, M.J., 2003. A rare earth element-rich carbonatite dyke at Bayan Obo, Inner Mongolia, North China. Mineralogy and Petrology 78, 93–110.
Yin, A., Harrison, T.M., 2000. Geologic evolution of the Himalayan–Tibetan orogen. Annual Review of Earth and Planetary Sciences 28, 211–280.
Yuan, Z.X., Bai, G., Wu, C.Y., 1992. Geological features and genesis of the Bayan Obo REE ore deposit, Inner Mongolia, China. Applied Geochemistry 7, 429–442.
Yuan, Z.X., Shi, Z.M., Bai, G., 1995. Rare Earth Element Deposit in Maoniuping, Mianning, Sichuan Province. Geological Publishing House, Beijing. (in Chinese).
Zartman, R.E., Doe, B.R., 1981. Plumebotectonics — the model. Tectonophys 75, 135–162.
Zhang, Y.X., Lu, Y.N., Yang, C.X., 1988. The Panxi rift. Geological Publishing House, Beijing, pp. 224–270 (in Chinese).
Zhang, Z.Q., Tang, S.H., Wang, J.H., Yuan, Z.X., Bai, G., 1994. New data for ore forming age of the Bayan Obo REE ore deposit, Inner Mongolia. Acta Geoscientica Sinica 1, 85–94 (in Chinese with English abstract).
Zhang, Z.Q., Tang, S.H., Yuan, Z.X., Bai, G., Wang, J.H., 2001. The Sm–Nd and Rb–Sr isotopic systems of the dolomites in the Bayan Obo ore deposit, Inner Mongolia, China. Acta Petrologica Sinica 17, 637–642 (in Chinese with English abstract).